The Astrophysical Journal, 836:159 (8pp), 2017 February 20 doi:10.3847/1538-4357/836/2/159

Revised Predictions of Neutrino Fluxes from Pulsar Wind Nebulae

Irene Di Palma[1,2], Dafne Guetta[3,4], and Elena Amato[5]
[1] Istituto Nazionale di Fisica Nucleare, Sezione di Roma, Italy; Irene.DiPalma@roma1.infn.it
[2] Universitá di Roma La Sapienza, I-00185 Roma, Italy
[3] INAF-Osservatorio Astronomico di Roma, v. Frascati 33, I-00040 Monte Porzio Catone, Italy; dafne.guetta@oa-roma.inaf.it
[4] Department of Physics Optical Engineering, ORT Braude, P.O. Box 78, Carmiel, Israel
[5] INAF-Osservatorio Astrofisico di Arcetri, Largo E. Fermi, 5, 50125, Firenze, Italy;
amato@arcetri.astro.it
Received 2016 April 20; revised 2016 July 20; accepted 2016 July 21; published 2017 February 16

Abstract

Several pulsar wind nebulae (PWN) have been detected in the TeV band in the last decade. TeV emission is typically interpreted in a purely leptonic scenario, but this often requires that the magnetic field in the nebula be much lower than the equipartition value, as well as the assumption of an enhanced density of target radiation at IR frequencies. In this work, we consider the possibility that, in addition to the relativistic electrons and positrons, relativistic hadrons are also present in these nebulae. Assuming that some of the emitted TeV photons are of hadronic origin, we compute the associated flux of ∼1–100 TeV neutrinos. We use IceCube non-detection to put constraints on the fraction of TeV photons that might be contributed by hadrons and estimate the number of neutrino events that can be expected from these sources in ANTARES and KM3Net.

Key words: gamma rays: ISM – ISM: supernova remnants – neutrinos

1. Introduction

Pulsar wind nebulae (PWN) are diffuse nebulae of non-thermal radiation, associated with the presence of a fast-spinning, strongly magnetized neutron star. The central star of a PWN may or may not be detected as a pulsar, but in either case it must emit what is called a pulsar wind—a relativistic magnetized outflow, primarily composed of electron–positron pairs. Confinement of this outflow by the surrounding supernova remnant or interstellar medium (ISM) leads to the formation of a termination shock, which slows the wind down to non-relativistic bulk speed. Particles are thereby accelerated to a power-law (or broken power-law) distribution. The interaction of these highly energetic leptons with the ambient magnetic field and the radio and IR background radiation is thought to be the origin of nebular emissions, from radio wavelengths to the TeV band. Since the discovery of the Crab Nebula, several other PWN have been discovered in the radio, optical, and X-ray bands (for a review, see Kargaltsev & Pavlov 2010). The Crab Nebula is the youngest and most energetic one.

As already mentioned, the material component of the wind primarily consists of electrons and positrons, due to the pair-production process that takes place in the star magnetosphere; however, a minority presence of ions cannot be excluded.

In spite of being minor in number, ions could still carry a dominant fraction of the total wind energy—helping explain how efficient acceleration of leptons is achieved at the pulsar wind termination shock (Hoshino et al. 1992; Amato & Arons 2006). For recent reviews on the subject, refer to Arons 2012 and Amato 2014.

Proofs of the presence of relativistic hadrons in PWN have been elusive so far, as for most astrophysical sources. In this particular environment, the most likely way in which hadrons would show their presence is through nuclear interactions that would lead to pion production. The following decay of neutral and charged pions would produce γ-rays and neutrinos, respectively, in the TeV range.

PWN are the most numerous sources of TeV photons in the Galaxy. Tens of such objects have been detected by TeV telescopes in the last decade, and many of the as-yet unidentified sources of GeV and TeV photons are suspected to be associated with a PWN.

The detected TeV emission is usually interpreted as the result of inverse Compton scattering (ICS) of the external radiation by the highly energetic electrons and positrons whose synchrotron emission is at the origin of lower-frequency nebular luminosity, from radio to X-rays and sometimes up to 10–100 MeV γ-rays. Reproducing the TeV emission within a purely leptonic model, however, often requires uncomfortable assumptions: the TeV flux often happens to be so large that, in order to interpret it as ICS, one needs to invoke a very weak magnetic field in the nebula, far below equipartition, and/or enhanced radio-IR background. These requirements would be largely alleviated if part of the TeV γ-rays were of hadronic origin. For a review on the role of hadrons in radiation processes of PWN, see (Cheng et al. 1990; Aharonian & Atoyan 1995).

In this work, we consider the possibility that part of the TeV emission is due to the decay of neutral pions produced in nuclear collisions. The same process that produces the neutral pions, and subsequently the TeV photons, would also generate charged pions that decay into neutrinos of similar energy. The IceCube high-energy neutrino telescope has been collecting data since 2006, and so far no neutrino event has been associated with a PWN. However, some of the nebulae with detected TeV emissions—according to the estimates of expected neutrino fluxes, based on the observed photon fluxes—are very promising already for the ANTARES detector, as well as for the upcoming neutrino Telescope KM3Net. We use IceCube non-detection to put constraints on the fraction of TeV photons that might be contributed by hadrons, as well as estimate the number of neutrino events that can be expected from these sources in ANTARES and in KM3Net.

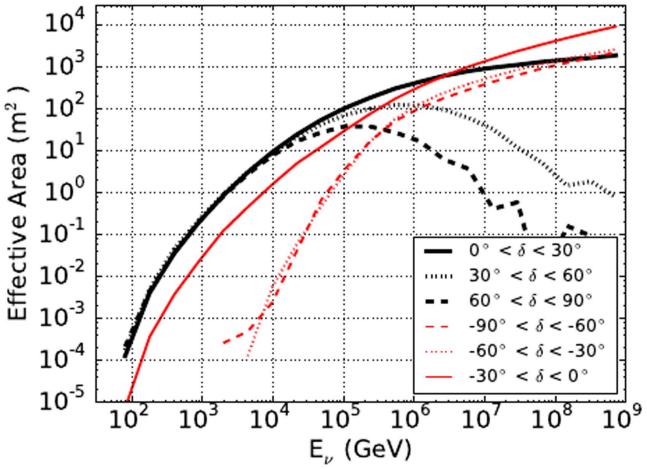

Figure 1. IceCube neutrino effective area for the 86-string configuration as a function of primary neutrino energy for six declination bands. The effective area is the average of the area for ν_μ and $\bar{\nu}_\mu$, Aartsen et al. (2014).

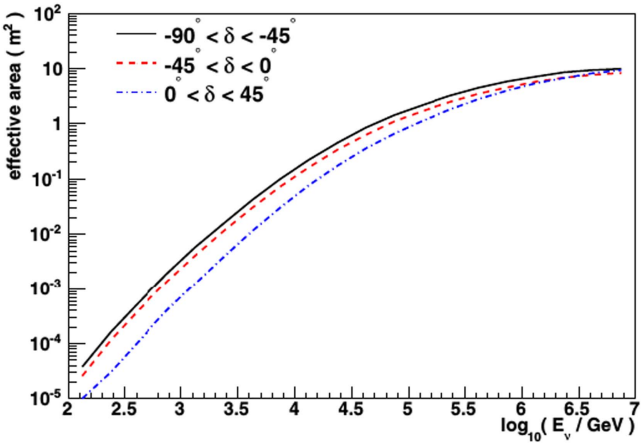

Figure 2. Effective area of the ANTARES detector for point sources, as a function of the neutrino energy for different declinations (Andrián-Martínez et al. 2012).

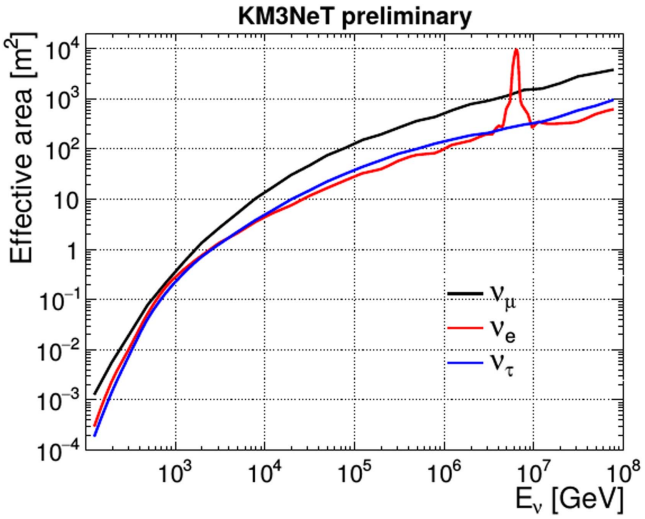

Figure 3. This plot is taken from Andrián-Martínez et al. (2016), it shows the effective areas of ARCA (two blocks) at trigger level for ν_μ, ν_e and ν_τ, as a function of neutrino energy E_ν. The effective area is defined relative to an isotropic neutrino flux incident on the Earth, is averaged over both ν and $\bar{\nu}$, and includes both NC and CC interactions. The peak at 6.3 PeV is due to the Glashow resonance of $\bar{\nu}_e$.

2. Neutrino Telescopes

High-energy neutrinos interact with nucleons present in the detector, producing secondary particles that travel faster than the speed of light in the sea or ice—and therefore induce the emission of Cherenkov radiation. Cherenkov photons are detected by optical sensors deployed in sea or ice. In the following, we briefly describe the basic characteristics of each telescope considered in this work.

IceCube, located at the geographic South Pole, is a cubic-kilometer particle detector buried in the Antarctic ice (Achterberg et al. 2006). Figure 1 displays the effective area of the 86-string configuration of the IceCube detector as a function of the neutrino energy for different values of declination.

The ANTARES detector is currently the only deep sea high energy neutrino telescope, which is operating in the Northern hemisphere Ageron et al. (2011). The telescope covers an area of about 0.1 km^2 on the sea bed, at a depth of 2475 m, 40 km off the coast of Toulon, France. Figure 2 shows the effective area of the ANTARES detector, with selection and reconstruction criteria optimized for the search of point like sources, as a function of the neutrino energy for different declinations Andrián-Martínez et al. (2012). ANTARES is planned to be followed by a multi-cubic-kilometer detector in the Mediterranean sea called KM3NeT in the next few years.

KM3Net (Andrián-Martínez et al. 2016) is the future generation of underwater neutrino telescopes. The infrastructure will consist of three so-called "building blocks," each made of 115 strings of 18 optical modules, with 31 photomultiplier tubes each. KM3Net consists of KM3Net/ARCA (Toulon, France) and KM3Net/ORCA (Capo Passero, Sicily). Figure 3 shows the effective area of KM3Net/ARCA as a function of the different neutrino flavors, ν_μ, ν_e, and ν_τ, at the trigger level (Andrián-Martínez et al. 2016). The calculation of the effective area includes the detector geometric acceptance, but not the efficiency of the apparatus and the effects of selection and reconstruction criteria.

3. TEV Observations of PWN

During the last few years, the number of PWN detected at TeV energies has increased from one (Weekes 1989) to 28. The current number of detected nebulae, mostly contributed by the H.E.S.S. survey of the Galactic plane (Carrigan et al. 2013), is similar to the number of these sources that are characterized at other frequencies. The Cherenkov Telescope Array (Actis et al. 2011) will likely increase this number to several hundred, probably providing an essentially complete account of TeV-emitting PWN in the Galaxy.

In Table 1, we list a collection of PWN that have been detected at multi-TeV photon energies, indicating for each of them the source declination, δ, the photon flux at 1 TeV, N_0, and the spectral index at TeV energies, α_γ, according to a description of the TeV photon spectrum in the form:

$$\frac{dN_\gamma}{dE_\gamma} = N_0 \left(\frac{E_\gamma}{1\ \mathrm{TeV}} \right)^{-\alpha_\gamma}, \quad (1)$$

where dN_γ/dE_γ is the number of photons per unit energy interval, time, and surface area.

As we mentioned in the introduction, a possible mechanism to interpret the TeV fluxes is the Inverse Compton Scattering

Table 1

Columns Indicate: the Name of the Source, its Declination, δ, in Degrees, the Number of 1 TeV Photons Per Unit Energy, Unit Time, and Unit Surface Detected from the Source, N_0 (See Equation (1)), the γ-Ray Spectral Index, α_γ, and the Reference from Which the Latter Two Values are Taken

Source Name	δ (°)	N_0 (10^{-11} TeV^{-1} cm^{-2} s^{-1})	Spectral Index	Reference
Crab	22.0145	2.8	−2.6	Aliu et al. (2008)
Vela	−45.17643	1.46	−1.32	Abramowski et al. (2012a)
MSH15-52	−59.1575	0.55	−2.21	Nakamori et al. (2008)
G54.1+0.3	18.86667	0.075	−2.39	Acciari et al. (2010)
G0.9+0.1	−28.15	0.084	−2.4	Aharonian et al. (2005a)
G21.5-0.9	−10.58333	0.046	−2.08	Djannati-Ataii (2008)
Kes75	2.983333	0.062	−2.26	Djannati-Ataii (2008)
J1356-645	−64.5	0.27	−2.2	Abramowski et al. (2011c)
CTA1	72.98361	0.102	−2.2	Aliu et al. (2013)
J1023-575	−57.79	0.33	−2.58	Abramowski et al. (2011a)
J1616-508	−50.9	0.67	−2.35	Aharonian et al. (2006c)
J1640-465	−46.53	0.3	−2.42	Aharonian et al. (2006c)
J1834-087	−8.76	0.26	−2.45	Aharonian et al. (2006c)
J1841-055	−5.55	1.28	−2.4	Aharonian et al. (2008)
J1813-178	−17.84	7.7	−2.09	Aharonian et al. (2006c)
J1632-478	−47.82	0.53	−2.12	Aharonian et al. (2006c)
J1458-608	−60.87722	0.21	−2.8	de los Reyes et al. (2012)
J1420-607	−60.76	0.35	−2.17	Aharonian et al. (2006a)
J1809-193	−19.3	0.46	−2.2	Aharonian et al. (2007)
J1418-609	−60.97528	0.26	−2.22	Aharonian et al. (2006a)
J1825-137	−13.83889	1.98	−2.38	Aharonian et al. (2006b)
J1831-098	−9.9	0.11	−2.1	Sheidaei et al. (2011)
J1303-631	−63.1775	0.59	−2.44	Abramowski et al. (2012b)
N 157B	−69.16583	0.13	−2.8	Abramowski et al. (2015)
J1837-069	−6.95	0.5	−2.27	Aharonian et al. (2006c)
J1912+101	+10.15167	0.35	−2.7	Aharonian et al. (2008)
J1708-443	−44.33333	0.42	−2.0	Abramowski et al. (2011b)

(ICS), on the ambient photon field of the electrons responsible for the synchrotron emission at lower frequencies. The target radiation for ICS might be composed, in general, of the sum of two different contributions: the external photon field; and the internal radiation produced by the source itself, typically lower-energy synchrotron emission by the same population of accelerated particles. In reality, however, the only source for which the internally produced photon field plays an important role is the Crab Nebula, which is absolutely exceptional because of its brightness as a synchrotron emitter. In all other cases, the photons that are upscattered in energy belong to the CMB or IR background. The latter is typically taken as the sum of two diluted blackbody spectra peaking in the far infrared, at $T_{\rm FIR} \approx 25$ K and in the near infrared, at $T_{\rm NIR} \approx 3000$ K (Porter et al. 2006). The energy density in the two components varies depending on their location in the Galaxy.

The ratio of the power emitted as ICS radiation to that emitted as synchrotron radiation by the same electrons provides an estimate of the ambient magnetic field, $B_{\rm ICS}$, if the energy density of the target radiation is known.

An independent estimate of the magnetic field can be obtained from the measurement of synchrotron emission alone, if some assumptions are made about the ratio between magnetic and particle energy density in the nebula. A common assumption is that of energy equipartition between the emitting particles and the magnetic field. In the following, we term $B_{\rm eq}$ the field strength derived under this assumption.

In the case of PWN that show a jet-torus morphology, such as Crab, Vela, and MSH15-52 (associated with PSR 1509-58), we expect that the magnetic field strength within the X-ray emitting nebula is not far from equipartition, because this is the condition required for jet formation (see Del Zanna et al. 2004). Therefore, the estimates of $B_{\rm eq}$ and $B_{\rm ICS}$ should result in similar values.

4. Neutrino Fluence Estimate

4.1. Expected Astrophysical Events

In this section, we compute the neutrino fluxes that would be expected from the TeV-detected PWN in IceCube, based on conversion of the whole photon flux in a corresponding number of neutrinos. We then discuss the most promising sources in some detail, and the implications of their non-detection by IceCube in terms of more refined predictions for ANTARES and KM3Net.

Relativistic protons may produce TeV γ-rays either by photo-meson production or inelastic nuclear collisions. In Guetta & Amato (2003), we showed that nuclear collisions are by far the most likely mechanism for pion production in PWN. The relation between the neutrino and photon fluxes is:

$$\int_{E_\nu^{\rm min}}^{E_\nu^{\rm max}} E_\nu \frac{dN_\nu}{dE_\nu} dE_\nu = \int_{E_\gamma^{\rm min}}^{E_\gamma^{\rm max}} E_\gamma \frac{dN_\gamma}{dE_\gamma} dE_\gamma \qquad (2)$$

where $E_\gamma^{\rm min}$ ($E_\nu^{\rm min}$) and $E_\gamma^{\rm max}$ ($E_\nu^{\rm max}$) are the minimum and maximum photon (neutrino) energies, respectively.

Such a simple rescaling of the γ-ray fluxes to the neutrino fluxes has been performed by Alvarez-Muniz & Halzen (2002) and Guetta & Amato (2003) for the Crab Nebula and for a few PWN observed in TeV γ-rays. We are aware that this is a

simplistic approximation, as most of the multiwavelegth photon emission from PWN seems to be due to leptonic processes rather than hadronic ones. However, it provides the most optimistic estimate of hadronic contribution to the TeV photon fluence measured by gamma-ray telescopes, and will be used as such.

We estimate the neutrino flux in the energy range 1–100 TeV, which is the range in which IceCube and ANTARES are operating—we assume the same range for KM3Net.

The total number of expected astrophysical events in a year of neutrino telescope operation is given by

$$N = \int_{1\ \mathrm{TeV}}^{100\ \mathrm{TeV}} T \frac{dN_\gamma}{dE_\gamma}(2E_\nu) A(E_\nu, \delta) dE_\nu \quad (3)$$

where T is the exposure time of one year, $\frac{dN_\gamma}{dE_\gamma}$ is the TeV spectrum (described according to Equation (1) with the parameters given in Table 1, according to the references reported in the table) and $A(E_\nu, \delta)$ is the effective area of the considered neutrino telescope, as a function of the neutrino energy E_ν and of the source declination, δ. We show $A(E_\nu, \delta)$ in Figures 1–3, for the IceCube, ANTARES, and KM3NeT/ARCA detectors respectively.

4.2. Expected Atmospheric Events

The main background component is the flux of atmospheric neutrinos, which is caused by the interaction of cosmic rays, high-energy protons, and nuclei with the Earth's atmosphere. Decay of charged pions and kaons produced in cosmic-ray interactions generates a flux of atmospheric neutrinos and muons. Their energy spectrum is about one power steeper than the spectrum of the parent cosmic rays at Earth, due to the energy-dependent competition between meson decay and interaction in the atmosphere. The spectral index for the cosmic ray power law is typically $\xi = 2.7$. For the following estimates, we do not consider the additional atmospheric component due to the decay of heavier mesons because it is relevant only for $E > 100$ TeV.

The atmospheric neutrino flux is expressed as a power law

$$\frac{d\Phi_\nu}{dE_\nu d\Omega} = C_\nu E_\nu^{-\beta} \quad (4)$$

where C_ν is a scale factor derived through Monte Carlo computations or experimental data, while $\beta \simeq \xi + 1$. The number of background neutrinos can be estimated as:

$$BG = \int_{1\ \mathrm{TeV}}^{100\ \mathrm{TeV}} T \frac{d\Phi_\nu}{dE_\nu d\Omega} A(E_\nu, \delta) dE_\nu\, d\Omega \quad (5)$$

where T is the exposure time of one year, $A(E_\nu, \delta)$ is the relative effective area we already discussed, and $\frac{d\Phi_\nu}{dE_\nu d\Omega}$ is the atmospheric neutrino flux. The latter is provided for ANTARES in Andrián-Martínez et al. (2013), and we use the same for KM3NeT/ARCA, whereas for IceCube we use the estimates given in Aartsen et al. (2015).

5. Neutrinos from PWN

In Table 2, we report the total number of PWN-associated neutrino events expected during one year of operation of the IceCube and ANTARES detectors, whereas in Table 3, the corresponding results are shown for KM3Net/ARCA. The number of atmospheric neutrino events collected in each detector is also reported. Because the dependence on declination of the effective area of KM3Net/ARCA is not yet available, the BG values are the same for each source in this case and only depend on the neutrino flavor. The neutrinos

Table 2
Predicted Neutrino Events from Each of the Considered PWN During One Year of Operation of IceCube and ANTARES

	IceCube		ANTARES	
Name	*N*	BG	*N*	BG
Crab	13.09	0.04	0.07	0.02
Vela	1.12	3.1e-07	4.33	0.06
MSH15-52	0.01	3.2e-07	0.09	0.06
G54.1+0.3	0.54	0.04	3.3e-3	0.02
G0.9+0.1	0.10	5.6e-3	7.8e-3	0.04
G21.5-0.9	0.13	5.6e-3	9.6e-3	0.04
Kes75	0.60	0.04	3.8e-3	0.02
J1356-645	8.4e-3	3.7e-06	0.05	0.06
CTA1	0.89	0.04	0.02	0.06
J1023-575	2.3e-3	3.2e-07	0.03	0.06
J1616-508	9.3e-3	3.2e-07	0.09	0.06
J1640-465	3.2e-3	3.2e-07	0.04	0.06
J1834-087	0.28	5.6e-3	0.02	0.04
J1841-055	1.53	5.64e-3	0.12	0.04
J1813-178	20.63	5.6e-3	1.56	0.04
J1632-478	0.018	3.2e-07	0.13	0.06
J1458-608	6.9e-4	3.7e-06	0.01	0.06
J1420-607	0.01	3.7e-06	0.07	0.06
J1809-193	0.9	5.6e-3	0.07	0.04
J1418-609	7.5e-3	3.7e-06	0.05	0.06
J1825-137	2.5	5.6e-3	0.19	0.04
J1831-098	0.29	5.6e-3	0.02	0.04
J1303-631	7.4e-3	3.7e-06	0.07	0.06
N 157B	4.3e-4	3.7e-06	7.3e-3	0.06
J1837-069	0.836	5.6e-3	0.06	0.04
J1912+101	1.366	0.04	7.4e-3	0.02
J1708-443	0.02	3.2e-07	0.11	0.04

Note. The first column lists the names of the sources; the second one reports the number of expected astrophysical neutrinos (left) and background neutrinos (right) for IceCube; the third one is the same as the second, but for ANTARES. The average angular resolution detector is taken to be $0.^\circ 6$ (Aartsen et al. 2014) for the IceCube detector, and $0.^\circ 46$ for ANTARES detector (Andrián-Martínez et al. 2012). The expected background events are computed in a sky patch of $3^\circ \times 3^\circ$ for both detectors.

Table 3
Results for the KM3Net/ARCA Detector

	KM3Net/ARCA		
Name	N_{ν_μ}	N_{ν_e}	N_{ν_τ}
Crab	25.29	8.51	9.46
Vela	345.96	79.60	105.91
MSH15-52	9.39	2.84	3.29
G54.1+0.3	0.99	0.31	0.36
G0.9+0.1	1.09	0.35	0.39
G21.5-0.9	1.21	0.34	0.41
Kes75	1.08	0.33	0.38
J1356-645	5.37	1.59	1.86
CTA1	2.03	0.60	0.70
J1023-575	3.37	1.11	1.24
J1616-508	9.67	3.00	3.45
J1640-465	3.77	1.11	1.36
J1834-087	3.08	0.99	1.12
J1841-055	16.72	5.28	6.02
J1813-178	197.84	56.26	67.12
J1632-478	12.68	3.64	4.33
J1458-608	1.38	0.49	0.53
J1420-607	7.46	2.18	2.57
J1809-193	9.157	2.70	3.17
J1418-609	4.95	1.47	1.72
J1825-137	26.91	8.44	9.64
J1831-098	2.76	0.79	0.94
J1303-631	7.13	2.28	2.59
N 157B	0.85	0.30	0.33
J1837-069	8.54	2.58	2.99
J1912+101	2.68	0.93	1.02
J1708-443	13.46	3.72	4.50

Note. The first column displays the name of the source; the second through fourth list the number of expected astrophysical events as a function of the different neutrino flavors ν_μ, ν_e, and ν_τ, considering a nominal angular resolution of $0^\circ.3$, (Aartsen et al. 2014). Because the effective area of KM3Net/ARCA is not given as a function of the declination, the BG values are the same for each source: $BG_{\nu_\mu} = 9.65$, $BG_{\nu_e} = 4.63$, and $BG_{\nu_\tau} = 4.64$, respectively. The expected background events are computed in a sky patch of $3^\circ \times 3^\circ$.

possibly produced in PWN would only be muons and electrons; however, due to the effective neutrino oscillations, an equal flux of all three flavors is expected in the detector.

The first thing that one notices when looking at Table 2 is that, by now, IceCube should have detected neutrinos from at least two sources: the Crab Nebula and J1813-178, if the entire γ-ray flux from those sources were of hadronic origin. Under the same assumption, a smaller—but still finite—number of events would have also been expected from a handful of other sources over the course of six years of integration with IceCube. The latter sources notably include Vela, which, as one can see from Table 3 and from the third column of Table 2, is the most promising candidate source for KM3Net and ANTARES. Indeed, although the number of neutrino events expected in IceCube is larger for J1813-178, when the computation is performed for the parameters appropriate for the next generation detectors (ANTARES and KM3Net), more neutrinos are expected from Vela, by a factor of two.

Further analyzing Tables 2 and 3, one notices that additional promising neutrino sources for ANTARES and KM3Net are, from top to bottom: MSH15-52, J1825-137, and J1841-055. Crab, Vela, and MSH15-52 have already been considered by Guetta & Amato (2003) as promising candidates for neutrino detection. These are well-studied PWN for which multi-wavelength data are available and spectral modeling has been developed by different authors. As mentioned above, these are also sources for which energy equipartition is believed to be a good approximation in the X-ray emitting nebula. In Table 4, we report, for each of these three sources, the magnetic field strength as estimated based on the equipartition argument applied to the X-ray emitting nebula ($B_{\rm eq}$ in column 7, based on the emission properties summarized in columns 2–6 of the same table), and the field strength that derives from high-energy spectral modeling ($B_{\rm ICS}$ in column 8). As we can see from this table, for 2 out of 3 sources, with Vela being the exception, the equipartition magnetic field is similar to what can be derived from the ICS. This can be taken as supporting evidence in favor of the dominant ICS origin of the TeV γ-ray flux from Crab and MSH15-52, albeit leaving room for a relevant hadronic contribution to the TeV flux from Vela.

6. Revised Neutrino Predictions in the Light of Icecube Results

In this section, we revise our prediction of the neutrino flux to be expected from our most promising sources, in light of their non-detection by IceCube. The neutrino flux is derived through considering the simple rescaling of γ-ray fluxes to the neutrino fluxes. For some of the sources discussed above, the fact that IceCube has detected no neutrinos for six years of integration implies, independent of any theoretical consideration, that the detected TeV γ-ray flux cannot be entirely of hadronic origin. Because, as can be seen from Table 2, the expected neutrino counts for one year of operation of IceCube are in all cases well above the background, we simply revise our estimate of the neutrino counts expected in ANTARES and KM3Net/ARCA by dividing the counts listed in column 3 of Table 2 (left-hand side) and in the three columns of Table 3 by $\max[1, 6N_{\rm ICE}]$ with $N_{\rm ICE}$ the counts listed in the second column of Table 2 (left-hand side). The results are reported in Table 5.

It is clear from the table that the most promising PWN to be detected by upcoming neutrino telescopes is Vela. At the same time, detection of neutrinos from MSH15-52 also appears possible, whereas the Crab Nebula is not expected to be observed. In the following section, we briefly comment on the likelihood of neutrino detection from the two best candidate neutrino sources, Vela and MSH15-52. In the case of the Crab Nebula, IceCube non-detection can be used to constrain the hadronic content of the pulsar wind—we briefly comment on

Table 4

Columns: Name of the Source (First Column); its X-Ray Luminosity (Second Column) Integrated in the Photon Energy Interval ϵ_1–ϵ_2 (Columns 3 and 4); Spectral Index (Column 5) Appropriate to Describe the X-Ray Emission as $F_\nu \propto \nu^{-\alpha_X}$ with F_ν, the Energy Emitted Per Unit Frequency, Time, Surface, and Steradian; the X-Ray Radius of the Nebula (Column 6) Approximated as a Sphere; the Equipartition Magnetic Field (Column 7) Estimated Based on the Specified X-Ray Emission Properties; the Strength of the Magnetic Field Derived from Spectral Modeling, Assuming that the γ-Ray Emission is All Due to ICS (Column 8) (see the Text for Further Details)

Source Name	L_X (10^{35} erg s^{-1})	ϵ_1 (keV)	ϵ_2 (keV)	α_X	$R_{\rm PWN}$ (pc)	$B_{\rm eq}$ (μG)	$B_{\rm ICS}$ (μG)
Crab	200	0.5	8	1.12	1.2	200	150
Vela	1.3×10^{-3}	0.5	8	0.4	0.1	25	5
MSH15-52	0.4	0.5	8	0.65	4.5	20	15

Table 5

Name of the Source (First Column); Revised Expectation of Neutrino Counts for One Year of Integration of ANTARES (Column 2); Revised Expectation for the Different Kinds of Neutrinos for KM3Net/ARCA

Source	ANTARES	KM3Net/ARCA		
	N_ν	N_{ν_μ}	N_{ν_e}	N_{ν_τ}
Crab	9×10^{-4}	0.3	0.1	0.12
Vela	0.64	51.48	11.85	15.76
MSH15-52	0.09	9.39	2.84	3.29
J1841-055	0.01	1.8	0.58	0.66
J1813-178	0.01	1.6	0.45	0.54
J1825-137	0.01	1.8	0.56	0.64

this, based on the results of Amato et al. (2003), deferring a more general and updated calculation to a forthcoming article.

7. Promising Candidate Neutrino Sources

7.1. Vela

The Vela PWN is the second-best studied PWN, after Crab. Data are available at basically all frequencies, but their interpretation is far more complicated than for Crab because this is an old and very complex system, where the emission of the PWN proper is not easy to disentangle from other contributions. Plenty of modeling is available, but the nature of the TeV emission is, in this case, more controversial. For example, Horns et al. (2006) suggest a most-likely hadronic origin of the TeV emission from Vela, mostly based on energetic arguments, whereas de Jager et al. (2008) and LaMassa et al. (2008) propose a fully leptonic model. In the light of the most recent release of Fermi data, Grondin et al. (2013) show that leptonic models can account well for the multiwavelength spectrum of the source with a magnetic field value of order 5 μG. It is interesting to note that, aside from a field well below equipartition, an enhanced IR photon field (a factor of five higher than the Galactic average) is required to explain TeV gamma-rays from Vela as ICS.

7.2. MSH15-52

MSH15-52 is the spectacular nebula produced by the pulsar PSR B1509-58, which is one of the youngest, most energetic pulsars known. It is 1700 year of age, with a 150 ms period and an estimated surface magnetic field of order 1.5×10^{13} G (Kaspi et al. 1994). The nebula has been observed in the radio and X-ray band (Gaensler et al. 2002), as well as in GeV (Abdo et al. 2010) and TeV (Aharonian et al. 2005b) γ-rays. Despite the morphological complexity of the system, thanks to the abundance of data, spectral modeling has been possible and the result is that the γ-ray flux of the source is well-explained with a magnetic field value very close to the equipartition one (17 μG versus 22 μG, Abdo et al. 2010). The main contribution to the target photon field for ICS comes from the IR background, that in this case is taken to be at the average Galactic level as inferred from GALPROP. It is important to mention that Abdo et al. (2010) have also attempted to interpret the γ-ray spectrum of this source as the result of π^0 decay: although the source is in a rather dense region, the energy that is required to be stored in relativistic protons—in order to explain the entire γ-ray flux as hadronic—exceeds the total energy supplied by the pulsar. Once again, this does not preclude the possibility that at least some of the high-energy photons are of hadronic origin. In terms of abundance of targets for nuclear collisions, this is one of the most promising sources.

7.3. The Crab Nebula

The Crab Nebula is the prototype PWN and one of the best-studied objects in the sky. It is a very bright source of photons at all energies, and used to be considered a calibration source for all high-energy telescopes, from X-rays to TeV γ-rays. The modeling of this source is obviously very well-developed and it is the only PWN so far for which spatially resolved modeling of both the dynamics and emission properties is available at all frequencies (see Amato 2014 for a review). A peculiarity of this source is that it is such a bright synchrotron emitter at all frequencies that its synchrotron radiation is a non-negligible target photon field for ICS. The field estimate obtained for $B_{\rm ICS}$ (e.g., de Jager & Harding 1992) is not far from the equipartition value, and the γ-ray spectrum of the source is accounted for reasonably well within a pure leptonic scenario (e.g., Meyer et al. 2010; Bucciantini et al. 2011).

It is appropriate to point out, however, that having the Crab Nebula's γ-ray emission well-explained as ICS does not mean that this source does not contain any relativistic hadrons, nor even that hadrons cannot be energetically dominant in the Crab pulsar wind. In fact, the latter condition could still be verified—the fact that we do not have any direct evidence for their presence in the γ-rays could be due either to the lack of target for p–p scattering, or just the fact that the leptonic emission is overwhelming. In the latter case, neutrino detection could still be possible and would provide the only available test for the presence of hadrons in the source.

Several models have been proposed for the γ-ray and neutrino production in the Crab Nebula, e.g., Bednarek & Protheroe (1997), Amato et al. (2003), Bednarek (2003), and Bednarek & Bartosik (2003). Those models describe, in detail, the physical parameters that are expected to determine the neutrino flux at different stages during the evolution of the nebula—most of them predict a flux of neutrinos corresponding to a few events per year in IceCube (see Bednarek et al. 2005

for a review) for the case in which hadrons carried most of the Crab pulsar wind energy flux. It is, therefore, clear that the IceCube non-detection can be used to put constraints on existing models of the Crab pulsar wind composition.

In Amato et al. (2003), the authors estimate the flux of neutrinos that could be expected from the direction of the Crab Nebula under the assumption that relativistic hadrons, with an energy distribution sharply peaked around the pulsar wind Lorentz factor, carried most of the wind energy. The number of predicted neutrinos was found to depend on the assumed wind Lorentz factor and target density in the nebula. According to that calculation, in the case of a wind with Lorentz factor $\approx$ a few $\times 10^6$ and 60% of the energy carried by hadrons, $\approx$10 neutrinos per year were expected to be detected in IceCube, for a target density corresponding to 10 $M_\odot$ of ejecta material uniformly distributed in the nebula (Hester 2008). The fact that IceCube has not detected any neutrinos from Crab seems to suggest that less than 15% of the wind energy is carried by hadrons, if the target density can be assumed as described above. However, a more refined calculation is needed to really assess the matter, one that also takes into account the fact that the spectrum of the ions might differ from the assumed monoenergetic distribution. This will be the subject of future work.

8. Summary and Conclusions

We have investigated the implications of a possible hadronic origin of the high-energy emission from PWN that have been detected at TeV energies.[6] The alternative explanation for this emission is purely leptonic (based on ICS). In reality, both leptons and hadrons could contribute to the emission, and their relative contributions affect the predictions for upcoming neutrino telescopes. Interesting constraints come, for some of the sources, from the non-detection by IceCube. We have devoted special attention to three sources: the Crab Nebula, and two other sources from which the neutrino number counts in upcoming detectors were found to be especially high when assuming that their entire TeV photon flux had a hadronic origin: Vela and MSH15-52.

In the case of the Crab Nebula, it is clear that the TeV γ-ray flux is mostly contributed by ICS, with at most a few percent of TeV photons deriving from hadronic processes. Because most models assuming ion dominance in the Crab pulsar wind also predict a finite number of neutrino events per year, the existing upper limits on the neutrino flux derived from IceCube non-detection can be used to put constraints on the hadronic content of the Crab pulsar wind. Based on the modelization by Amato et al. (2003), we derive an upper limit of about 15% on the fraction of pulsar wind energy carried by hadrons if the wind Lorentz factor is a few $\times 10^6$ and the target density corresponds to $10 M_\odot$ of material uniformly distributed in the nebula. The downside is that Crab has an unfavorable declination for the upcoming neutrino telescopes, and not much progress in this area is expected from their operation.

The second source we considered, Vela, turns out to be the best candidate PWN to be detected in neutrinos. Even taking into account the IceCube non-detection, the revised number of expected neutrinos still suggests that the source could be detected by ANTARES within a few years of integration and promptly by KM3Net/ARCA. We also mentioned the difficulties associated with a fully leptonic interpretation of the γ-ray flux from this source: namely, the requirement that the nebular magnetic field be on average a factor of five below the estimated equipartition field and the presence of an enhanced IR background. Taking into account all this, Vela really appears to be a promising neutrino source.

A detectable neutrino flux is also expected from MSH15-52, whereas for the remaining potentially promising sources in our list, the IceCube constraints strongly reduce the perspectives of detection with the KM3Net detector.

It is important to note that the KM3Net/ARCA predictions were derived without considering the effect of the efficiency of the apparatus and the selection and reconstruction criteria.

The Cherenkov Telescope Array will likely increase the number of PWN detected at TeV energy to several hundreds, probably providing an essentially complete account of TeV-emitting PWN in the Galaxy. The analysis performed in this work can be easily extended to each upcoming TeV-detected PWN.

The authors gratefully acknowledge the support of this research by the Italian Istituto Nazionale di Fisica Nucleare and L'Oréal Italia For Women in Science.

[6] www.asdc.asi.it/tgevcat/

References

Aartsen, M. G., Ackermann, M., Adams, J., et al. 2014, ApJ, 796, 109
Aartsen, M. G., Ackermann, M., Adams, J., et al. 2015, PhRvD, 91, 122004
Abdo, A. A., Ackermann, M., Ajello, M., et al. Fermi coll. 2010, ApJ, 714, 927
Abramowski, Acero, F., Aharonian, F., et al. 2011b, A&A, 528, A143
Abramowski, A., Acero, F., Aharonian, F., et al. 2011a, A&A, 525, A46
Abramowski, A., Acero, F., Aharonian, F., et al. 2011c, A&A, 533, A103
Abramowski, A., Acero, F., Aharonian, F., et al. 2012a, A&A, 548, A38
Abramowski, A., Acero, F., Aharonian, F., et al. 2012b, A&A, 548, A46
Abramowski, A., Aharonian, F., Ait Benkhali, F., et al. 2015, Science, 347, 406
Acciari, V. A., Aliu, E., Arlen, T., et al. 2010, ApJL, 719, L69
Achterberg, A., Ackermann, M., Adams, J., et al. (IceCube Collaboration) 2006, APh, 26, 155
Actis, M., Agentta, F., Aharonian, F., et al. 2011, ExA, 32, 193
Ageron, M., Aguilar, J. A., Al Samarai, I., et al. 2011, NIMPA, 656, 11
Aharonian, F., & Atoyan, A. 1995, APh, 3, 275
Aharonian, F., Akhperjanian, A. G., Aye, K.-M., et al. 2005a, A&A, 432, L25
Aharonian, F., Akhperjanian, A. G., Bazer-Bachi, A. R., et al. 2005b, A&A, 435, L17
Aharonian, F., Akhperjanian, A. G., Bazer-Bachi, A. R., (HESS Collaboration) et al. 2006a, A&A, 456, 245
Aharonian, F., Akhperjanian, A. G., Bazer-Bachi, A. R., et al. 2006b, ApJ, 636, 777
Aharonian, F., Akhperjanian, A. G., Bazer-Bachi, A. R., et al. 2006c, A&A, 460, 365
Aharonian, F., Akhperjanian, A. G., Bazer-Bachi, A. R., et al. 2007, A&A, 472, 489
Aharonian, F., Akhperjanian, A. G., Barres de Almeida, U., et al. 2008, A&A, 477, 353
Aharonian, F., Akhperjanian, A. G., Aye, K.-M., et al. 2005a, A&A, 432, L25
Aliu, E., Anderhub, H., Antonelli, L. A., et al. 2008, Sci, 322, 1222
Aliu, E., Archambault, S., Arlen, T., et al. 2013, ApJ, 764, 38
Alvarez-Muniz, J., & Halzen, F. 2002, ApJL, 576, L33
Amato, E. 2014, IJMPS, 28, 1460160
Amato, E., & Arons, J. 2006, ApJ, 653, 325
Amato, E., Guetta, D., & Blasi, P. 2003, A&A, 402, 827
Andrián-Martínez, S., Samarai, I., Albert, A., et al. 2012, ApJ, 760, 53
Andrián-Martínez, S., Albert, A., Al Samarai, I., et al. 2013, EPJC, 73, 2606
Andrián-Martínez, S., Ageron, M., Aharonian, A., et al. 2016, arXiv:1601.07459
Arons, J. 2012, SSRv, 173, 341
Bednarek, W. 2003, A&A, 407, 1
Bednarek, W., & Bartosik, M. 2003, A&A, 405, 689
Bednarek, W., Burgio, G. F., & Montaruli, T. 2005, NewAR, 49, 1
Bednarek, W., & Protheroe, R. J. 1997, PhRvL, 79, 2616

Bucciantini, N., Arons, J., & Amato, E. 2011, MNRAS, 410, 381
Carrigan, S., Brun, F., Chaves, R. C. G., et al. 2013, in Proc. 33rd ICRC, Rio de Janeiro, Brazil, arXiv:1307.4690v3
Cheng, K. S., Cheung, T., Lau, M. M., Yu, K. N., & Kwok, P. W. 1990, JPhG, 16, 1115
de Jager, O. C., & Harding, A. K. 1992, ApJ, 396, 161
de Jager, O. C., Slane, P. O., & LaMassa, S. 2008, ApJL, 689, 125
Del Zanna, L., Amato, E., & Bucciantini, N. 2004, A&A, 423, 253
Djannati-Ataii, A., de Jager, O. C., Terrier, R., Gallant, Y. A., & Hoppe, S. in Proc. 30th ICRC, Merida, Mexico, 2, 823, arXiv:0710.2247
Gaensler, B. M., Arons, J., Kaspi, V. M., et al. 2002, ApJ, 569, 878
Grondin, M.-H., Romani, R. W., Lemoine-Goumard, M., et al. 2013, ApJ, 774, 110
Guetta, D., & Amato, E. 2003, APh, 19, 403
Hester, J. J. 2008, ARA&A, 46, 127
Honda, M., Kajita, T., Kasahara, K., Midorikawa, S., & Sanuki, T. 2007, Phys. Rev., D, 75, 043006
Horns, D., Aharonian, F., Santangelo, A., Hoffmann, A. I. D., & Masterson, C. 2006, A&A, 451, 51
Hoshino, M., Arons, J., Gallant, Y., & Langdon, A. B. 1992, ApJ, 390, 454
Kargaltsev, O., & Pavlov, G. G. 2010, in AIP Conf. Proc. 1248, X-Ray Astronomy; Present Status, Multi-wavelength Approach and Future Perspectives, ed. A. Comastri, L. Angelini, & M. Cappi (Melville, NY: AIP), 25
Kaspi, V. M., Manchester, R. N., Siegman, B., Johnston, S., & Lyne, A. G. 1994, ApJL, 422, L83
LaMassa, S., Slane, P. O., & de Jager, O. C. 2008, ApJL, 689, 121
Meyer, M., Horns, D., & Zechlin, H.-S. 2010, A&A, 523, 11
Nakamori, T., Kubo, H., Yoshida, T., et al. 2008, ApJ, 677, 297
Porter, T., Moskalenko, I. V., & Strong, A. W. 2006, ApJL, 648, 29
de los Reyes, Zajczyk, A., Chaves, R. C. G., et al. 2011, in Proc. 32th ICRC, Beijing, China, arXiv:1205.0719
Sheidaei, F., Djannati-Ataï, A., Gast, H., et al. 2011, in Proc. 32th ICRC, Beijing, China, arXiv:1110.6837
Torres, D. F., Cillis, A., Martìn, J., & de Ona Wilhelmi, E. 2014, JHEAp, 1, 31
Weekes, T. 1989, ApJ, 342, 379

The Astrophysical Journal, 848:74 (4pp), 2017 October 10 https://doi.org/10.3847/1538-4357/aa8a65

Erratum: "Revised Predictions of Neutrino Fluxes from Pulsar Wind Nebulae" (2017, ApJ, 836, 159)

Irene Di Palma[1,2], Dafne Guetta[3,4], and Elena Amato[5,6]
[1] Istituto Nazionale di Fisica Nucleare, Sezione di Roma, Italy; Irene.DiPalma@roma1.infn.it
[2] Universitá di Roma La Sapienza, I-00185 Roma, Italy
[3] Istituto Nazionale di Astrofisica—Osservatorio astronomico di Roma, v. Frascati 33, I-00040 Monte Porzio Catone, Italy; dafne.guetta@oa-roma.inaf.it
[4] Department of Physics Optical Engineering, ORT Braude, P.O. Box 78, Carmiel, Israel
[5] Istituto Nazionale di Astrofisica—Osservatorio Astrofisico di Arcetri, Largo E. Fermi, 5, I-50125, Firenze, Italy; amato@arcetri.astro.it
[6] Dipartimento di Fisica e Astronima—Università degli Studi di Firenze, Via Sansone, 1, I-50019—Sesto Fiorentino (FI), Italy
Received 2017 August 5; revised 2017 September 1; published 2017 October 12

1. Introduction

This is an erratum to correct the work published in Di Palma et al. (2017), with the title "Revised Predictions of Neutrino Fluxes from Pulsar Wind Nebulae." Members of the ANTARES Collaboration, to whom we are very grateful, pointed out issues with the estimates of neutrino fluxes and backgrounds that were provided in that work. After double checking our estimates and discussing with members of both the ANTARES and IceCube Collaborations, we are prompted to revise the contents of that article.

In the above mentioned work, we were estimating the expected neutrino flux from a collection of pulsar wind nebulae (PWNe) observed in very high-energy gamma-rays. We computed the expected neutrino flux from each of the sources in the 2 existing neutrino telescopes, IceCube and ANTARES, and in the upcoming KM3NeT, assuming that their entire gamma-ray flux above 1 TeV is of hadronic origin. The comparison of the computed flux with the relevant background, again computed theoretically, showed that a handful of objects in our list of sources should have already been detected by IceCube if all their gamma-ray emission derived from hadronic processes. The lack of detection was then turned into an upper limit on the fraction of γ-rays that could come from hadrons and in a revised estimate of the flux of neutrinos expected from these sources in ANTARES and KM3NeT.

The published work contained important flaws. We list them in the following and provide corrections.

Table 1
List of PWNe that Were Considered in the Original Article

Source Name	δ [°]	N_0 [10^{-11} TeV^{-1} cm^{-2} s^{-1}]	spectral index	reference
Crab	22.015	2.8	−2.6	Aharonian et al. 2004
Vela	−45.18	1.46	−1.32	Abramowski et al. 2012a
MSH15-52	−59.24	0.52	−2.21	Nakamori et al. (2008)
G54.1+0.3	18.87	0.075	−2.39	Acciari et al. (2010)
G0.9+0.1	−28.15	0.084	−2.4	Aharonian et al. (2005)
G21.5-0.9	−10.56	0.046	−2.08	Djannati-Ataii et al. (2008)
Kes75	−2.98	0.062	−2.26	Djannati-Ataii et al. (2008)
J1356-645	−64.5	0.27	−2.2	Abramowski et al. (2011b)
CTA1	72.98	0.102	−2.2	Aliu et al. (2013)
J1023-575	−57.79	0.33	−2.58	Abramowski et al. (2011a)
J1616-508	−50.90	0.67	−2.35	Aharonian et al. (2006a)
J1640-465	−46.53	0.3	−2.42	Aharonian et al. (2006a)
J1834-087	−8.76	0.26	−2.45	Aharonian et al. (2006a)
J1841-055	−5.55	1.28	−2.4	Aharonian et al. (2008a)
J1813-178	−17.84	0.27	−2.09	Aharonian et al. (2006a)
J1632-478	−47.82	0.53	−2.12	Aharonian et al. (2006a)
J1458-608	−60.88	0.21	−2.8	de los Reyes et al. (2012)
J1420-607	−60.76	0.35	−2.17	Aharonian et al. (2006b)
J1809-193	−19.30	0.46	−2.2	Aharonian et al. (2007)
J1418-609	−60.975	0.26	−2.22	Aharonian et al. (2006b)
J1825-137	−13.84	1.98	−2.38	Aharonian et al. (2006c)
J1831-098	−9.90	0.11	−2.1	Sheidaei et al. (2011)
J1303-631	−63.18	0.59	−2.44	Abramowski et al. (2012b)
N 157B	−69.17	0.13	−2.8	Abramowski et al. (2015)
J1837-069	−6.95	0.5	−2.27	Aharonian et al. (2006a)
J1912+101	+10.15	0.35	−2.7	Aharonian et al. (2008b)
J1708-443	−44.33	0.42	−2.0	Abramowski et al. (2011c)

Table 2
Amended Estimates of the Astrophysical Neutrinos for the Sources Listed in Table 1. The Number of Background Neutrinos Is Independent on Declination $N_{BG} = 0.42$. Corrected Version of Table 2 of the Original Article

ANTARES	
Source	N_ν
Crab	6.19×10^{-3}
Vela No Cut-Off	0.94
Vela with Cut-off	0.068
MSH15-52	0.012
G54.1+0.3	3.3×10^{-4}
G0.9+0.1	8.07×10^{-4}
G21.5-0.9	1.23×10^{-3}
Kes75	9.18×10^{-4}
J1356-645	6.45×10^{-3}
CTA 1	8.67×10^{-4}
J1023-575	2.57×10^{-3}
J1616-508	0.01
J1640-465	3.66×10^{-3}
J1834-087	2.15×10^{-3}
J1841-055	1.19×10^{-2}
J1813-178	6.92×10^{-3}
J1632-478	0.016
J1458-608	9.31×10^{-4}
J1420-607	9.26×10^{-3}
J1809-193	8.27×10^{-3}
J1418-609	5.85×10^{-3}
J1825- 137	0.02
J1831-098	2.76×10^{-3}
J1303-631	6.79×10^{-3}
N 157B	5.76×10^{-4}
J1837-069	7.17×10^{-3}
J1912+101	6.08×10^{-4}
J1708-443	0.015

2. Conversion of γ-ray Fluxes into Neutrino Fluxes

The conversion of the high energy photon flux into a neutrino flux was wrong by a factor between 5 and 8 depending on the source, due to a mistake in the calculation of the integral:

$$N_\nu = T \int_{1\mathrm{TeV}}^{100\mathrm{TeV}} dE_\nu \; \Phi_0 \; \times (2E_\nu)^{-\Gamma} \; \times A_{\mathrm{eff}}(\delta, E_\nu), \tag{1}$$

where T is the integration time and E_ν is the neutrino energy in TeV. A corrected version of Tables 2 and 3 of Di Palma et al. (2017) is provided in Tables 2, 3, and 4 below.

We also report, in Table 1, a corrected version of the Table 1 of Di Palma et al. (2017) where we correct a flux that was wrongly reported and a reference (for source J1912+101 we refer now to Aharonian et al. 2008b).

3. Estimate of the Background

In Di Palma et al. (2017), the background was theoretically estimated as

$$N_{\mathrm{BG}} = T \int_{1\mathrm{TeV}}^{100\mathrm{TeV}} dE_\nu \; \Phi_{\nu,atm}(E_\nu) \; \times A_{\mathrm{eff}}(\delta, E_\nu), \tag{2}$$

with

$$\Phi_{\nu,atm}(E_\nu) = 12 \times 10^{-11} E_\nu^{-3.4} \; \mathrm{cm}^{-2}\,\mathrm{s}^{-1}\,\mathrm{TeV}^{-1}. \tag{3}$$

However, both the ANTARES Collaboration and the IceCube Collaboration found that our estimates were too optimistic.

For ANTARES, we have been advised to always use the maximum effective area when computing the background and also use 200 GeV as the lower limit of integration rather than 1 TeV. We then replace 1 TeV with 200 GeV and A_{eff} with $A_{\mathrm{eff,max}}$ in Equation (2), where $A_{\mathrm{eff,max}}$ corresponds to the largest effective area, relative to the declinations $-90^\circ < \delta < 45^\circ$, and corresponds to the black solid curve in Figure 2 of Di Palma et al. (2017). Revised estimates are reported in the second column of Table 2.

Table 3
Amended Estimates of the Astrophysical Neutrinos and Background for the Sources Listed in Table 1. Corrected Version of Table 2 of the Original Article. First Column: Name of the Source; Second Column: Number of Neutrinos Expected from that Specific Astrophysical Source; Column 3: Number of Background Neutrinos in 1° of Sky in One Year, Estimated Using the Integral from 1 TeV and Using the Effective Area Corresponding to that Specific Declination; Column 4: Number of Background Neutrinos Measured by IceCube, as Reported by Aartsen et al. (2017)

	IceCube		
Source	N_ν	$N_{\rm BG}$ theor	$N_{\rm BG}$ meas
Crab	2.66	2.6	9.4
Vela no Cut-off	0.65	6.4×10^{-4}	6.54
Vela with Cut-off	4.55×10^{-3}	6.4×10^{-4}	6.54
MSH15-52	3.93×10^{-3}	6.4×10^{-4}	6.4
G54.1+0.3	0.13	2.6	9.9
G0.9+0.1	0.024	0.37	7.4
G21.5-0.9	0.038	0.37	7.4
Kes75	0.028	0.37	6.8
J1356-645	$2.76 \times 10 - 3$	9.3×10^{-4}	6.05
CTA1	0.24	2.4	5.42
J1023-575	4.83×10^{-4}	6.4×10^{-4}	6.63
J1616-508	2.70×10^{-3}	6.4×10^{-4}	6.63
J1640-465	8.87×10^{-4}	6.4×10^{-4}	6.7
J1834-087	0.065	0.37	7.07
J1841-055	0.36	0.37	7.07
J1813-178	0.21	0.37	7.5
J1632-478	5.97×10^{-3}	6.4×10^{-4} 3	6.38
J1458-608	1.52×10^{-4}	9.3×10^{-4}	6.25
J1420-607	4.093×10^{-3}	9.3×10^{-4}	6.25
J1809-193	0.25	0.37	7.54
J1418-609	2.42×10^{-3}	9.3×10^{-4}	6.2
J1825-137	0.61	0.37	7.47
J1831-098	0.084	0.37	7.17
J1303-631	2.05×10^{-3}	9.3×10^{-4}	6.1
N 157B	9.43×10^{-5}	9.3×10^{-4}	6.05
J1837-069	0.22	0.37	7.57
J1912+101	0.27	2.6	10.45
J1708-443	8.14×10^{-3}	6.4×10^{-4}	6.52

As far as IceCube is concerned, a comparison of our published background estimates (computed according to Equation (2)), with the work of Aartsen et al. (2017), shows a large discrepancy, which is partly due to the fact that IceCube cannot eliminate completely background events below 1 TeV, where the atmospheric flux is large. Our discussion with members of the IceCube Collaboration convinced us that the most appropriate thing to do is to use the actual IceCube measurements of the background as a function of the declination, as they are provided by Aartsen et al. (2017). The corrected numbers are reported in column 4 of Table 3.

In both Tables 2 and 3, the Vela PWN appears twice. The two different estimates are associated with different assumptions on the Vela gamma-ray emission spectrum. The difference between the two depends on if one takes into account the fact that the Vela gamma-ray emission spectrum seems to cut off at 14 TeV as found by Abramowski et al. (2012a). If such a cut-off is taken into account the estimated number of neutrinos corresponds to the second entry in the Tables.

Based on the amended estimates of astrophysical and background neutrino fluxes, no sources are now above IceCube background. Therefore, IceCube non-detection does not provide any constraint on the fraction of TeV gamma-rays from PWNe that can be of hadronic origin. As a result, the calculations leading to the updated neutrino predictions reported in Table 5 of the original article loose significance: present day data do not allow us to put any constraint on the fraction of the gamma-ray flux observed from PWNe that can be of hadronic origin.

In Table 2, we report the number of neutrinos detectable from the source and the background for ANTARES. The number of background neutrinos for ANTARES is always the same independent on declination $N_{\rm BG} = 0.42$.

In Table 3, we report the number of neutrinos detectable from the source and the background for IceCube. In the third column of the table, we report the number of background neutrinos for IceCube computed according to Equation (2), while in the fourth column the number of background events as measured by Aartsen et al. (2017) is reported. We notice that the number of background events reported in the fourth column of Table 3, while much larger than our theoretical estimate for all the sources, are not very different from what can be estimated adopting for IceCube a procedure similar to that adopted for ANTARES, which is namely using the maximum effective area independently of the source declination and integrating in energy from 200 GeV rather than from 1 TeV.

In Table 4, we report the number of neutrinos of different types that could be expected from each of the considered sources in KM3NeT.

Also this number is lower than what was found in Di Palma et al. (2017).

Table 4

Corrected Results for the KM3NeT/ARCA Detector. The First Column Displays the Name of the Source, while Columns 2, 3 and 4 Report the Number of Expected Astrophysical Events for the Different Neutrino Flavors ν_μ, ν_e and ν_τ, Considering a Nominal Angular Resolution of 0.3°. Since the Effective Area of KM3NeT/ARCA Is Not Given as Function of the Declination, the BG Values Are the Same for Each Source and Are, Respectively: $BG_{\nu_\mu} = 18.4$, $BG_{\nu_e} = 46.6$, $BG_{\nu_\tau} = 19.3$. The Expected Background Events Are Computed in a Sky Patch of $3° \times 3°$

KM3NeT			
Source	N_{ν_e}	N_{ν_μ}	N_{ν_τ}
Crab	1.59	4.80	1.77
Vela no Cut-Off	35.44	155.93	47.54
Vela with Cut-Off	5.13	16.52	5.83
MSH15-52	0.75	2.57	0.88
G54.1+0.3	0.069	0.22	0.079
G0.9+0.1	0.076	0.25	0.087
G21.5-0.9	0.092	0.33	0.11
Kes75	0.079	0.26	0.091
J1356-645	0.39	1.37	0.47
CTA1	0.15	0.52	0.18
J1023-575	0.20	0.61	0.23
J1616-508	0.68	2.23	0.79
J1640-465	0.26	0.83	0.30
J1834-087	0.21	0.67	0.24
J1841-055	1.13	3.64	1.29
J1813-178	0.52	1.87	0.63
J1632-478	0.96	3.39	1.15
J1458-608	0.08	0.24	0.091
J1420-607	0.55	1.93	0.66
J1809-193	0.67	2.33	0.79
J1418-609	0.36	1.24	0.43
J1825-137	1.87	6.09	2.15
J1831-098	0.21	0.75	0.25
J1303-631	0.49	1.55	0.56
N 157B	0.05	0.15	0.056
J1837-069	0.61	2.07	0.72
J1912+101	0.17	0.49	0.18
J1708-443	1.06	3.89	1.29

We would like to thank Dorothea Samtleben who helped us to understand that part of our published fluxes were wrong; we thank also Maurizio Spurio and Francis Halzen who helped us with the estimate of the neutrino background for Antares and IceCube, respectively.

ORCID iDs

Elena Amato https://orcid.org/0000-0002-9881-8112

References

Aartsen, M. G., Abraham, K., Ackermann, M., et al. 2017, ApJ, 835, 15
Abramowski, A., Acero, F., Aharonian, F., et al. 2011a, A&A, 525, A46
Abramowski, A., Acero, F., Aharonian, F., et al. 2011b, A&A, 533, A103
Abramowski, A., Acero, F., Aharonian, F., et al. 2011c, A&A, 528, A143
Abramowski, A., Acero, F., Aharonian, F., et al. H.E.S.S. Collaboration 2012a, A&A, 548, A38
Abramowski, A., Acero, F., Aharonian, F., et al. 2012b, A&A, 548, A46
Abramowski, A., Aharonian, F., Ait Benkjali, F., et al. 2015, Sci, 347, 406
Acciari, V. A., Aliu, E., Arlen, T., et al. 2010, ApJ, 719, L69
Aharonian, F., Akhperjanian, A., Beilicke, M., et al. 2004, ApJ, 614, 897
Aharonian, F., Akhperjanian, A. G., Aye, K.-M., et al. 2005, A&A, 432, L25
Aharonian, F., Akhperjanian, A. G., Bazer-Bachi, A. R., et al. 2006a, ApJ, 636, 777
Aharonian, F., Akhperjanian, A. G., Bazer-Bachi, A. R., et al. 2006b, A&A, 456, 245
Aharonian, F., Akhperjanian, A. G., Bazer-Bachi, A. R., et al. 2006c, A&A, 460, 365
Aharonian, F., Akhperjanian, A. G., Bazer-Bachi, A. R., et al. H.E.S.S. Collaboration 2007, A&A, 472, 489
Aharonian, F., Akhperjanian, A. G., Barres de Almeida, U., et al. H.E.S.S. Collaboration 2008a, A&A, 477, 353
Aharonian, F., Akhperjanian, A. G., Barres de Almeida, U., et al. H.E.S.S. Collaboration 2008b, A&A, 484, 435
Aliu, E., Archambault, S., Arlen, T., et al. VERITAS Collaboration 2013, ApJ, 764, 38
Di Palma, I., Guetta, D., & Amato, E. 2017, ApJ, 836, 159
Djannati-Ataii, A., de Jager, O. C., Terrier, R., Gallant, Y. A., & Hoppe, S. 2008, Proc. ICRC, 30, in press (arXiv:0710.2247)
de los Reyes, R., Zajczyk, A., & Chaves, R. C. G. 2012, Proc. ICRC, 32, (arXiv1205.0719)
Nakamori, T., Kubo, H., Yoshida, T., et al. 2008, ApJ, 677, 297
Sheidaei, F., Djannati-Atai, A., & Gast, H. 2012, Proc. ICRC, 32, 1125